

Fully self-consistent optimization of the Jastrow-Slater-type wave function using a similarity-transformed Hamiltonian

Masayuki Ochi

Department of Physics, Osaka University, Machikaneyama-cho, Toyonaka, Osaka 560-0043, Japan

(Dated: September 14, 2021)

For highly accurate electronic structure calculation, the Jastrow correlation factor is known to successfully capture the electron correlation effects. Thus, the efficient optimization of the many-body wave function including the Jastrow correlation factor is of great importance. For this purpose, the transcorrelated + variational Monte Carlo (TC+VMC) method is one of the promising methods, where the one-electron orbitals in the Slater determinant and the Jastrow factor are self-consistently optimized in the TC and VMC methods, respectively. In particular, the TC method is based on similarity-transformation of the Hamiltonian by the Jastrow factor, which enables efficient optimization of the one-electron orbitals under the effective interactions. In this study, by test calculation of a helium atom, we find that the total energy is systematically improved by using better Jastrow functions, which can be naturally understood by considering a role of the Jastrow factor and the effective potential introduced by the similarity-transformation. We also find that one can partially receive a benefit of the orbital optimization even by one-shot TC+VMC, where the Jastrow parameters are optimized at the Hartree-Fock+VMC level, while a quality of the many-body wave function is inferior to that for self-consistent TC+VMC. A difference between TC and biorthogonal TC is also discussed. Our study provides important knowledge for optimizing many-body wave function including the Jastrow correlation factor, which would be of great help for development of highly accurate electronic structure calculation.

PACS numbers:

I. INTRODUCTION

Accurate description of the electronic structure relies on whether the theory captures essential aspects of the electron correlation effects. One important aspect of many-electron correlation originates from the singular behavior of the Coulomb interaction at electron coalescence points, which is represented with the Kato cusp condition [1, 2]. From this viewpoint, an explicit inclusion of the electron-electron distance r_{12} into the theory is crucial, as pointed out in pioneering works by Hylleraas [3–5]. It is now well known that, a slow convergence with respect to the basis-set size for one-electron orbitals is effectively improved by the R12 [6] and F12 [7] theories.

Because the R12 and F12 theories aim to an efficient approach to the complete-basis-set (CBS) limit, the CBS limit itself is unchanged by the use of r_{12} -dependent functions. Another attempting idea is to improve the accuracy of the wave function by including the two-electron variables into the wave function. A representative example is the Jastrow-Slater-type wave function, where the Jastrow factor, which depends on r_{12} and often more complicated coordinates, is multiplied by the Slater determinant. Quantum Monte Carlo (QMC) methods, such as the variational Monte Carlo (VMC) and diffusion Monte Carlo methods [8], successfully handle this kind of wave functions not only for atoms and molecules but also for condensed matters [9]. A key point here is that evaluation of physical quantities for the many-body wave function including the Jastrow factor requires a $3N$ -dimensional integration (N : the number of electrons), which is efficiently performed with the Monte Carlo technique.

An alternative way to handle the Jastrow factor is introduced by Boys and Handy [10, 11]: they proposed to use the Hamiltonian similarity-transformed by the Jastrow factor. Then, orbital optimization for the Jastrow-Slater-type wave function is regarded as the Hartree-Fock (HF) approximation to the similarity-transformed Hamiltonian, which does not require a huge-dimensional integration mentioned above. This is called the transcorrelated (TC) method [10–14]. An important advantage of the TC method is that one can apply sophisticated post-HF methods to the similarity-transformed Hamiltonian. To say, the TC method can be a promising starting point of the wave-function theory instead of HF; electron correlation effects are partially taken into account already at the first hierarchy level with respect to the similarity-transformed Hamiltonian. In fact, previous studies performed TC calculations combined with the couple-cluster theory [15], Möller-Plesset (MP) perturbation theory [12, 13], and configuration interaction (CI) theory [16–19] for atomic and molecular systems. Canonical TC method [20] is an important development, in which one employs the idea of the similarity transformation in the context of the F12 theory. Recently, the canonical TC method was used in conjunction with the variational quantum eigensolver method [21]. Also, it is remarkable that the canonical TC method efficiently reduces the number of required Slater determinants in the full-CI QMC calculation [22, 23]. A recent study that combines the TC method with the quantum computational method is also promising [24]. Moreover, an efficient treatment of the correlation effects enables one to apply the TC method to solids [25–29], including its combination with the CI-singles [30] and the second-order

MP perturbation theory [31]. The TC and related methods were also applied to the Hubbard model [32–35], electron gas [25, 36–39], one-dimensional quantum gas with contact interactions [40], and ultracold atoms [41].

Quantum-chemical theories mainly focus on improvement over the Slater determinant. On the other hand, optimizing the Jastrow factor is another important way to improve the quality of the many-body wave function. While a parameter-free (i.e. no degree of freedom for optimization) Jastrow function sometimes works well (e.g. [12, 19, 25, 37]), parameters in the Jastrow factor have been successfully optimized in the TC method [14, 17, 18, 27, 38, 42, 43]. However, Jastrow optimization in the TC method still has not been well investigated: how it affects the accuracy of the total energy and the pseudoenergy, which is an expectation value of the similarity-transformed Hamiltonian, what is the efficient way for optimization, how the effective interactions in the similarity-transformed Hamiltonian are altered by Jastrow optimization, and so on. It is noteworthy that a recent study by Cohen *et al.* sheds light on the importance of the Jastrow optimization in the TC method [44]. While their study uses the Jastrow parameters optimized for the HF orbitals, fully self-consistent optimization of both the Jastrow factor and the Slater determinant is desired. The full optimization of the Jastrow-Slater-type wave function is also challenging for QMC calculation [45, 46].

In this study, we systematically investigate the fully self-consistent solution of the TC method, where both the Jastrow factor and the Slater determinant are optimized. We use the TC+VMC method [14] because VMC is a well-established method for optimizing the Jastrow factor in the Jastrow-Slater-type wave function, using more sophisticated Jastrow functions compared to the previous study of the TC+VMC method [14]. We investigate both the TC and biorthogonal TC (BiTC) methods, where the left and right Slater determinants can be different. Although many previous studies investigate one of these two formulations, we find that the pseudoenergy is much different between two formulations. To understand the nature of the similarity transformation, we also investigate how the effective interactions in the similarity-transformed Hamiltonian are altered by Jastrow optimization. We perform these calculations on a helium atom, which is one of the simplest many-electron systems, but offers a rich knowledge of electron correlation effects. We take a sufficiently large number of basis functions for one-electron orbitals to eliminate the basis-set error and see how the correlation effects are described in the optimized Jastrow factor. We find that the total energy is systematically improved by using better Jastrow functions, which can be naturally understood by considering the role of the Jastrow factor and the effective TC potential induced by it. By improving the Jastrow function, it is found that the expectation value of the non-Hermitian TC Hamiltonian (pseudoenergy) gets closer to that of the original Hamiltonian. These differ-

ent estimates of the total energy roughly coincide when one includes the electron-electron-nucleus terms into the Jastrow function. We also find that one can partially receive a benefit of the orbital optimization even by one-shot TC+VMC, where the Jastrow parameters are optimized at the HF+VMC level, while a quality of the many-body wave function is inferior to that for self-consistent TC+VMC. This study offers a great clue to know how one can efficiently improve a quality of many-body wave function including the Jastrow correlation factor, which would be of great help for development of highly accurate electronic structure calculation.

The paper is organized as follows. In Sec. II, we briefly present a theoretical framework of the TC method. Our implementation of the all-electron TC calculation for the closed-shell atom is presented in Sec. III. In Sec. IV, we introduce the TC+VMC method and the Jastrow functions used in this study. Calculation results are shown in Sec. V. Section VI is devoted to the conclusion of this study. Hartree atomic units (a.u.) are used throughout this paper: $\hbar = |e| = m_e = 4\pi\varepsilon_0 = 1$.

II. TC METHOD

Here we briefly describe a theoretical framework of the TC method, a detail of which was presented in previous papers [10, 12, 14]. Hamiltonian \mathcal{H} for an N -electron system under the external potential $v_{\text{ext}}(x)$ is written as,

$$\mathcal{H} = \sum_{i=1}^N \left(-\frac{1}{2} \nabla_i^2 + v_{\text{ext}}(\mathbf{r}_i) \right) + \sum_{i=1}^N \sum_{j>i}^N \frac{1}{|\mathbf{r}_i - \mathbf{r}_j|}, \quad (1)$$

where $x = (\mathbf{r}, \sigma)$ denotes a set of spatial and spin coordinates associated with an electron. First, we formally factorize the many-body wave function Ψ as $\Psi = F\Phi$ where F is the Jastrow factor,

$$F = \exp\left(-\sum_{i,j(>i)}^N u(x_i, x_j)\right), \quad (2)$$

and Φ is defined as $\Phi \equiv \Psi/F$. Here we assume the Jastrow function $u(x_i, x_j)$ to be symmetric, i.e., $u(x_i, x_j) = u(x_j, x_i)$, without loss of generality. Next, we introduce a similarity-transformed Hamiltonian,

$$\mathcal{H}_{\text{TC}} \equiv F^{-1} \mathcal{H} F, \quad (3)$$

by which the Schrödinger equation is rewritten as,

$$\mathcal{H}\Psi = E\Psi \Leftrightarrow \mathcal{H}_{\text{TC}}\Phi = E\Phi. \quad (4)$$

In this way, electron correlation effects described with the Jastrow factor are incorporated into the similarity-transformed Hamiltonian \mathcal{H}_{TC} , which we called the TC

Hamiltonian hereafter. \mathcal{H}_{TC} can be explicitly written as,

$$\begin{aligned} \mathcal{H}_{\text{TC}} = & \sum_{i=1}^N \left(-\frac{1}{2} \nabla_i^2 + v_{\text{ext}}(\mathbf{r}_i) \right) + \sum_{i=1}^N \sum_{j>i}^N v_{2\text{body}}(x_1, x_2) \\ & - \sum_{i=1}^N \sum_{j>i}^N \sum_{k>j}^N v_{3\text{body}}(x_1, x_2, x_3), \end{aligned} \quad (5)$$

where $v_{2\text{body}}(x_1, x_2)$ and $v_{3\text{body}}(x_1, x_2, x_3)$ are the effective interactions in the TC Hamiltonian defined as,

$$\begin{aligned} & v_{2\text{body}}(x_1, x_2) \\ \equiv & \frac{1}{|\mathbf{r}_1 - \mathbf{r}_2|} + \frac{1}{2} \left[\nabla_1^2 u(x_1, x_2) + \nabla_2^2 u(x_1, x_2) \right. \\ & \left. - (\nabla_1 u(x_1, x_2))^2 - (\nabla_2 u(x_1, x_2))^2 \right] \\ & + \nabla_1 u(x_1, x_2) \cdot \nabla_1 + \nabla_2 u(x_1, x_2) \cdot \nabla_2, \end{aligned} \quad (6)$$

and

$$\begin{aligned} & v_{3\text{body}}(x_1, x_2, x_3) \\ \equiv & \nabla_1 u(x_1, x_2) \cdot \nabla_1 u(x_1, x_3) + \nabla_2 u(x_2, x_1) \cdot \nabla_2 u(x_2, x_3) \\ & + \nabla_3 u(x_3, x_1) \cdot \nabla_3 u(x_3, x_2). \end{aligned} \quad (7)$$

By approximating Φ to be a single Slater determinant consisting of one-electron orbitals: $\Phi = \det[\phi_i(x_j)]$, the following one-body self-consistent-field (SCF) equation is derived (e.g., see [14]):

$$\begin{aligned} & \left(-\frac{1}{2} \nabla_1^2 + v_{\text{ext}}(\mathbf{r}_1) \right) \phi_i(\mathbf{r}_1) \\ & + \sum_{j=1}^N \int d\mathbf{r}_2 \phi_j^*(\mathbf{r}_2) v_{2\text{body}}(x_1, x_2) \det \begin{bmatrix} \phi_i(\mathbf{r}_1) \phi_i(\mathbf{r}_2) \\ \phi_j(\mathbf{r}_1) \phi_j(\mathbf{r}_2) \end{bmatrix} \\ & - \sum_{j=1}^N \sum_{k>j}^N \int d\mathbf{r}_2 d\mathbf{r}_3 \phi_j^*(\mathbf{r}_2) \phi_k^*(\mathbf{r}_3) v_{3\text{body}}(x_1, x_2, x_3) \\ & \times \det \begin{bmatrix} \phi_i(\mathbf{r}_1) \phi_i(\mathbf{r}_2) \phi_i(\mathbf{r}_3) \\ \phi_j(\mathbf{r}_1) \phi_j(\mathbf{r}_2) \phi_j(\mathbf{r}_3) \\ \phi_k(\mathbf{r}_1) \phi_k(\mathbf{r}_2) \phi_k(\mathbf{r}_3) \end{bmatrix} = \sum_{j=1}^N \epsilon_{ij} \phi_j(\mathbf{r}_1), \end{aligned} \quad (8)$$

where the orthonormal condition, $\langle \phi_i | \phi_j \rangle = \delta_{i,j}$, is imposed. The TC one-electron orbitals $\phi_i(\mathbf{r})$ are optimized by solving Eq. (8). Φ can be systematically improved over a single Slater determinant by applying the post-HF theories to the similarity-transformed Hamiltonian [12, 13, 15, 30, 31], which is an important advantage of the TC method. This feature is validated by the equivalency between the two eigenvalue problems presented in Eq. (4): to say, the exact eigenstate of the original Hamiltonian \mathcal{H} can be immediately constructed from the exact eigenstate of \mathcal{H}_{TC} by $\Psi = F\Phi$. In this study, however, we concentrate on the case when Φ is approximated as a single Slater determinant.

The total energy,

$$E = \frac{\langle \Psi | \mathcal{H} | \Psi \rangle}{\langle \Psi | \Psi \rangle}, \quad (9)$$

equals to the TC pseudoenergy,

$$E_{\text{TC}} = \text{Re} \left[\frac{\langle \Phi | \mathcal{H}_{\text{TC}} | \Phi \rangle}{\langle \Phi | \Phi \rangle} \right], \quad (10)$$

when Φ is the exact eigenstate of \mathcal{H}_{TC} . While this is of course not true for an approximate Φ , we can still approximately evaluate the total energy by E_{TC} , which does not require N -dimensional integration. For example, when Φ is a single Slater determinant, E_{TC} can be calculated by 9-dimensional (three-body) integration. This is another great advantage of the TC method from the viewpoint of computational cost. However, accuracy of the approximation $E_{\text{TC}} \simeq E$ should be carefully checked, which is one of the main objectives of this study.

We also mention the biorthogonal formulation of the TC method, which we called the BiTC method. The BiTC method was applied to molecules [13] and recently also to solids [31]. A detailed description of the BiTC method can be found in these literatures. In the BiTC method, we use left and right Slater determinants consisting of different one-electron orbitals: $X = \det[\chi_i(x_j)]$ and $\Phi = \det[\phi_i(x_j)]$, respectively, with the biorthogonal condition $\langle \chi_i | \phi_j \rangle = \delta_{i,j}$ and the normalization condition $\langle \phi_i | \phi_i \rangle = 1$. Then a one-body SCF equation becomes slightly different from Eq. (8) in the sense that $\phi^*(x)$ are replaced with $\chi^*(x)$. The BiTC pseudoenergy is defined as,

$$E_{\text{BiTC}} = \text{Re} \left[\frac{\langle X | \mathcal{H}_{\text{TC}} | \Phi \rangle}{\langle X | \Phi \rangle} \right]. \quad (11)$$

Because the similarity transformation of Hamiltonian introduces non-Hermiticity, such formulation yields a different result from the ordinary TC method presented above. A difference between the TC and BiTC methods is also an issue that we shall investigate in this paper.

III. ALL-ELECTRON TC CALCULATION FOR AN ATOM

Here we describe how we perform the all-electron calculation of the TC method. In this study, we focus on the non-relativistic treatment of the closed-shell atom with a nucleus charge Z placed at the origin.

A. One-electron orbitals and a basis set

We represent the left and right one-electron orbitals by the spherical harmonics Y_{l_i, m_i} and the radial functions as follows:

$$\phi_{n_i, l_i, m_i, \sigma_i}(\mathbf{r}) = Y_{l_i m_i}(\Omega) \frac{\phi_{n_i, l_i, \sigma_i}^{\text{rad}}(r)}{r}, \quad (12)$$

$$\chi_{n_i, l_i, m_i, \sigma_i}(\mathbf{r}) = Y_{l_i m_i}(\Omega') \frac{\chi_{n_i, l_i, \sigma_i}^{\text{rad}}(r)}{r}, \quad (13)$$

where n_i, l_i, m_i, σ_i denote the principal, azimuthal, magnetic, and spin quantum numbers, respectively. We often abbreviate $\phi_{n_i, l_i, \sigma_i}^{\text{rad}}$ as ϕ_i^{rad} hereafter. We expand the radial functions with the azimuthal quantum number l_i using a following basis function (see, e.g. [49, 50]):

$$f_n^{l_i}(r) = (2\alpha)^{l_i+\frac{3}{2}} \sqrt{\frac{n!}{(n+2l_i+2)!}} r^{l_i+1} L_n^{(2l_i+2)}(2\alpha r) e^{-\alpha r}, \quad (14)$$

where $\alpha = \sqrt{-2\epsilon_{\text{HO}}}$ is a scaling factor and $L_n^{(k)}$ is an associated Laguerre polynomial:

$$L_n^{(k)}(x) \equiv \frac{e^x x^{-k}}{n!} \frac{d^n}{dx^n} (e^{-x} x^{n+k}), \quad (15)$$

some examples of which are $L_0^{(k)}(x) = 1$, $L_1^{(k)}(x) = -x + k + 1$, and so on. This basis function satisfies correct asymptotic behaviors of the radial function [51]: $f_n^{l_i}(r) \rightarrow e^{-\alpha r}$ for $r \rightarrow \infty$ and $f_n^{l_i}(r) \rightarrow r^{l_i+1}$ for $r \rightarrow 0$. Hence, any orbitals that can be represented by a product of $r^{l_i+1} e^{-\alpha r}$ and a polynomial of r can be expanded with this basis set. Orthonormality of this basis set is readily verified (see Appendix A). Note that the scaling factor α is updated in each SCF loop because it depends on the eigenenergy of the highest occupied orbitals, ϵ_{HO} [53].

B. TC-SCF equation for the radial function

The TC-SCF equation for the radial function of the right orbitals reads

$$\left[-\frac{1}{2} \frac{d^2}{dr^2} + \frac{l_i(l_i+1)}{2r^2} + \hat{V}[\phi, \chi] \right] \phi_i^{\text{rad}}(r) = \sum_j^N \epsilon_{ij} \phi_j^{\text{rad}}(r), \quad (16)$$

where \hat{V} denotes the one-, two-, and three-body potentials as described in more detail later in this paper. Equations for the left orbitals can be obtained in the same way and so are not shown here.

We solved the TC-SCF equation (16) by evaluating the matrix elements of the left-hand side of this equation with respect to the basis functions defined in Eq. (14), and diagonalizing the matrix [54, 55]. Since we assume that the one-electron orbital is a product of the spherical harmonics and radial function, diagonalization is separately performed for each (l, m, σ) . This procedure is repeated until the self-consistency with respect to the orbitals is achieved, because $\hat{V}[\phi, \chi]$ depends on the orbitals ϕ and χ . The matrix elements are evaluated on the real-space grid points. To describe a rapid oscillation of the wave functions near a nucleus, we used a log mesh $\rho = \ln(r)$ for the real-space grid. We applied a sufficiently large cutoff for the range of ρ with the boundary condition that ϕ^{rad} and χ^{rad} go to zero at the both end points.

C. One-body terms in the TC-SCF equation

A matrix element for the one-body terms in the TC-SCF equation (16),

$$\int_0^\infty f_m^{l_i}(r) \left[-\frac{1}{2} \frac{d^2}{dr^2} + \frac{l_i(l_i+1)}{2r^2} - \frac{Z}{r} \right] f_n^{l_i}(r) dr, \quad (17)$$

can be rewritten as follows (see Appendix B):

$$-\frac{\alpha^2}{2} \delta_{m,n} + \left(-Z + \alpha \frac{(l_i+1)(2l_i+2\min(m,n)+3)}{2l_i+3} \right) \int_0^\infty f_m^{l_i}(r) \frac{1}{r} f_n^{l_i}(r) dr, \quad (18)$$

and we numerically evaluated the integral $\langle f_m^{l_i} | 1/r | f_n^{l_i} \rangle$. By using a log mesh, $dr = r d\rho$ removes a diverging behavior ($1/r$) of the integrand.

If one includes a one-body Jastrow function, a one-body effective potential will appear in the similarity-transformed Hamiltonian. In this study, we did not include any one-body Jastrow function in the TC calculation, because this is a duplicated degree of freedom with one-electron orbitals. To say, a one-body Jastrow function is not necessary when one optimizes one-electron orbitals.

Nevertheless, we here make few notes for including the one-body Jastrow function, because it can be a useful

way for some purposes, e.g., for imposing the (nucleus-electron) cusp condition on the one-body Jastrow function instead of the one-electron orbitals. One-body effective potentials can be easily obtained by substituting the one-body Jastrow function for Eqs. (6)-(7). For using a one-body Jastrow function, one should properly change a basis set of the one-electron orbitals, Eq. (14), because an asymptotic behavior of the one-electron orbitals can be altered by the Jastrow factor. Regarding this point, we note that the localizing property of the one-electron orbitals near a nucleus can be lost depending on the one-body Jastrow function, which can induce numerical difficulty in solving the TC-SCF equation. Thus, it will

be better to properly restrict the degree of freedom of the one-body Jastrow function even if one would like to include it in the TC calculation.

D. Two- and three-body terms in the TC-SCF equation

The one-body terms in the TC-SCF equation, Eq. (16), are easily evaluated because they come down to the one-dimensional integral of the smooth function. However, the two- and three-body terms require higher-dimensional integration, involving the angle coordinates of the orbitals appearing in $\hat{V}[\phi, \chi]$. In this study, we performed Monte Carlo integration for the two- and three-body terms in the TC-SCF equation for simplicity.

The Monte Carlo sampling is performed in the following procedure. We go back to the SCF equation, Eq. (8), and define the two-body matrix element as

$$\langle F_{n_1}^{lm} | v_{2\text{body}} | F_{n_2}^{lm} \rangle \equiv \sum_{j=1}^N \int d\mathbf{r}_1 d\mathbf{r}_2 (F_{n_1}^{lm}(\mathbf{r}_1))^* \phi_j^*(\mathbf{r}_2) \\ \times v_{2\text{body}}(x_1, x_2) \det \begin{bmatrix} F_{n_2}^{lm}(\mathbf{r}_1) F_{n_2}^{lm}(\mathbf{r}_2) \\ \phi_j(\mathbf{r}_1) \phi_j(\mathbf{r}_2) \end{bmatrix}, \quad (19)$$

where

$$F_n^{l,m}(\mathbf{r}) = Y_{lm}(\Omega_1) \frac{f_n^l(r_1)}{r_1} \quad (20)$$

is a basis function of the orbitals. Since we assume that the one-electron orbital is a product of the spherical harmonics and the radial function, we only consider the diagonal matrix element of the quantum numbers (l, m, σ) , while all occupied (l_j, m_j, σ_j) are summed over for the state j . $\langle F_{n_1}^{lm} | v_{2\text{body}} | F_{n_2}^{lm} \rangle$ can be regarded as a two-body part of $\langle f_{n_1}^l | \hat{V}[\phi, \chi] | f_{n_2}^l \rangle$. Monte Carlo sampling for Eq. (19) is performed in the $(\mathbf{r}_1, \mathbf{r}_2)$ space. Because we can fix $\phi_2 = 0$ by symmetry of the orbitals, five-dimensional integration is required. Evaluation of the three-body terms can be done in the same way, which requires eight-dimensional integration.

We note that the two-body terms like $\nabla_1 u(x_1, x_2) \cdot \nabla_1 \phi_i(\mathbf{r}_1)$ depend on the gradient of the orbital. For handling these terms, we used

$$\nabla \phi_i(\mathbf{r}) = \left(-\frac{\phi_i^{\text{rad}}(r)}{r^2} + \frac{1}{r} \frac{d\phi_i^{\text{rad}}(r)}{dr} \right) Y_{l_i m_i}(\Omega) \mathbf{e}_r \\ + \frac{\phi_i^{\text{rad}}(r)}{r^2} \left(\frac{\partial Y_{l_i m_i}(\Omega)}{\partial \theta} \mathbf{e}_\theta + \frac{im_i}{\sin \theta} Y_{l_i m_i}(\Omega) \mathbf{e}_\varphi \right), \quad (21)$$

and the following formula (see Appendix C),

$$\frac{\partial Y_{l_i m_i}(\Omega)}{\partial \theta} = sgn(m_i) \sqrt{(l_i - |m_i|)(l_i + |m_i| + 1)} Y_{l_i, m_i + sgn(m_i)}(\Omega) e^{-isgn(m_i)\varphi} + |m_i| \frac{\cos \theta}{\sin \theta} Y_{l_i, m_i}(\Omega), \quad (22)$$

where $sgn(m_i) = +1$ ($m_i \geq 0$), -1 ($m_i < 0$), for evaluating the derivative of the spherical harmonics. For evaluating the derivative of the radial functions in Eq. (21), we simply adopted the finite-difference method.

We note that the Jacobian $r^2 \sin \theta$ removes the diverging function ($1/r$ and $1/\sin \theta$) in Eq. (21) and other potential terms, by which numerical difficulty is avoided. Derivative of the Jastrow function in the effective potentials presenting in Eqs. (6)-(7) are evaluated analytically (see Appendix D). The Jastrow function used in this study shall be shown in Section IV A.

IV. TC+VMC METHOD

By performing the TC calculation presented in Section III, one can optimize the one-electron orbitals for a given Jastrow function. To optimize the Jastrow function for given one-electron orbitals, we performed the VMC calculation. In the VMC calculation, one minimizes the

total energy, Eq. (9), or the variance,

$$\sigma^2 = \frac{\langle \Psi | (\mathcal{H} - E_{\text{VMC}})^2 | \Psi \rangle}{\langle \Psi | \Psi \rangle}, \quad (23)$$

which are evaluated with the Monte Carlo integration. Hereafter, VMC calculation with the energy-minimization and that with the variance-minimization are denoted by ‘emin’ and ‘varmin’, respectively. In this paper, we do not describe technical details of VMC, and instead refer the readers to a review article [8].

In the TC+VMC method, one repeats the TC and VMC calculations alternately for optimizing both the one-electron orbitals and the Jastrow function. We stopped this iteration when one finds that the additional VMC calculation no longer improves the Jastrow function.

We should mention a small difference between our TC+VMC calculation and that studied by Umezawa *et al.* [14] In Ref. [14], the variance defined for the TC

Hamiltonian,

$$\sigma_{\text{TC}}^2 = \frac{\langle \Phi | (\mathcal{H}_{\text{TC}}^\dagger - E_{\text{TC}})(\mathcal{H}_{\text{TC}} - E_{\text{TC}}) | \Phi \rangle}{\langle \Phi | \Phi \rangle}, \quad (24)$$

is minimized instead of σ^2 . Both guiding principles should work because both of σ^2 and σ_{TC}^2 become zero for the exact ground state. We shall briefly discuss their difference in Section V.

A. Jastrow functions used in this study

The Jastrow function used in this study is as follows:

$$u(x_1, x_2) = \sum_{(i,j,k) \in S} c_{ijk}^{\sigma_1 \sigma_2} \bar{r}_{12}^i \bar{r}_1^j \bar{r}_2^k, \quad (25)$$

where S is a combination of (i, j, k) considered in this Jastrow function, and \bar{r}_{12} and \bar{r}_i ($i = 1, 2$) are defined as,

$$\bar{r}_{12} = \frac{r_{12}}{r_{12} + a_{12}}, \quad \bar{r}_i = \frac{r_i}{r_i + a} \quad (i = 1, 2), \quad (26)$$

with $r_{12} = |\mathbf{r}_1 - \mathbf{r}_2|$. This Jastrow function is often used in VMC studies [56, 57]. For simplicity, we set $a_{12} = a$. Since u is a symmetric function, $c_{ijk}^{\sigma_1 \sigma_2} = c_{ikj}^{\sigma_1 \sigma_2}$ is imposed. We also assume $c_{ijk}^{\uparrow\uparrow} = c_{ijk}^{\downarrow\downarrow}$ and $c_{ijk}^{\uparrow\downarrow} = c_{ijk}^{\downarrow\uparrow}$ since we consider non-spin-polarized atoms here. For satisfying the cusp conditions [1, 2], we set

$$c_{100}^{\uparrow\uparrow} = c_{100}^{\downarrow\downarrow} = \frac{a_{12}}{4}, \quad c_{100}^{\uparrow\downarrow} = c_{100}^{\downarrow\uparrow} = \frac{a_{12}}{2}. \quad (27)$$

and $c_{1jk}^{\sigma_1 \sigma_2} = 0$ except $j = k = 0$ for simplicity. We also imposed $c_{i1k}^{\sigma_1 \sigma_2} = c_{ij1}^{\sigma_1 \sigma_2} = 0$ since our one-electron orbitals satisfy the nucleus cusp condition, and $c_{000}^{\sigma_1 \sigma_2} = 0$ since this component plays no role in improving a quality of the wave function.

In this study, we investigate the following three cases:

- $S_{\text{minimum}} = \{(1, 0, 0)\}$,
- $S_{\text{ee}} = \{(i, 0, 0) | 1 \leq i \leq 4\}$,
- $S_{\text{seen}} = S_{\text{ee}} \cup \{(0, 2, 2), (2, 2, 0), (2, 0, 2), (2, 2, 2)\}$.

S_{minimum} represents the minimum Jastrow function satisfying the cusp conditions, which only has a one free parameter a . S_{ee} corresponds to an electron-electron Jastrow function, and few electron-electron-nucleus terms are added for S_{seen} . One-body Jastrow functions, $(i, j, k) = (0, j, 0)$ and $(0, 0, k)$, were not included in this study because of the reasons explained in Section III C.

V. RESULTS

In this paper, we applied the TC+VMC method to a helium atom as a test case. While a helium atom can be regarded as one of the simplest “many-body” problem, it includes essential aspects of the electron correlation effects. We also used the BiTC method, as described in the following sections.

A. Computational details

For the HF and (Bi)TC calculations, a radial mesh for one-electron orbitals was set in the range of e^{-9} Bohr $\leq r \leq e^6$ Bohr. Within this range, a log mesh with $N_{\text{mesh}} = 80,000$ was taken in the HF and (Bi)TC calculations, while 500 times coarser grid (i.e., $N_{\text{mesh}} = 160$) was used as an input orbital for VMC for efficient Monte Carlo sampling in VMC. The number of mesh for each angle coordinate was 5,000. The number of Monte Carlo sampling in the integral calculations of the HF and (Bi)TC methods was 2.56 billions for each SCF iteration. These large numbers might be improved by efficient implementation of the Monte Carlo sampling, while it is not the scope of this study. The number of SCF cycles was set to 30. Since it is not easy to judge whether the self-consistency is reached because of the statistical error, we estimated the total energy as a statistical average for the last 10 SCF loops in the way described later in this section. Jastrow functions described in Sec. IV A were used. For a helium atom, only the Jastrow function for the antiparallel spin pairs is required except when one calculates the unoccupied orbitals and their energies. For calculating the unoccupied states, we set the spin-parallel Jastrow parameters to be the same as those for the spin-antiparallel Jastrow parameters, except c_{100} determined by the cusp condition.

For the VMC calculation, we used CASINO code [58]. We performed both the energy minimization and the variance minimization for the Jastrow-parameter optimization, and compared them in the following sections. We took at most 800 millions of Monte Carlo steps and 40 cycles for each optimization. These relatively large values are required because of the high sensitivity of the (Bi)TC results on the Jastrow parameters as we shall see later.

For the TC+VMC self-consistent loops, we judged that the self-consistency is reached when the Jastrow parameters are not optimized further. To say, the energy (variance) is not lowered for the energy- (variance-) optimization in further VMC calculations. Typically 10–20 iterations were required to reach the self-consistency between the TC and VMC calculations.

We show the VMC energy with an error bar estimated by the CASINO code. For the HF and (Bi)TC methods, we calculated the standard error of the total energies for the last 10 SCF iterations of the HF and (Bi)TC calculations, and show it as an estimated error for the Monte Carlo sampling and the self-consistency within the HF and (Bi)TC calculations.

In the TC+VMC method, we can use both the TC and BiTC methods in the orbital optimization. However, for a helium atom, we found that the right one-electron orbitals are almost the same between the TC and BiTC methods as long as the same Jastrow factor is used. Thus, in this study, we optimized the one-electron orbitals by the TC method until the TC+VMC self-consistent loop is converged, and finally evaluated E_{TC} and E_{BiTC} using

the optimized Jastrow function by performing the TC and BiTC calculations. We also found that the imaginary part of the orbitals and eigenvalues are negligibly small for a helium atom, and also for other closed-shell atoms in our preliminary calculation. At the moment, we only numerically verified this and do not have a proof for it, which is an important future issue.

Note that one-electron orbitals used in VMC calculation should be orthonormalized (see [55] for theoretical detail of the orthonormalization in the (Bi)TC calculation). Thus, we should perform Gram-Schmidt orthonormalization also for the BiTC orbitals if one would like to use the BiTC orbitals as an input for VMC calculations, while the orthonormalized orbitals are not used in the BiTC calculation itself. This kind of orthogonalization is validated by the invariance of the Slater determinant against a linear combination within the occupied orbitals.

B. Convergence with respect to the number of basis functions

We first checked convergence with respect to the number of basis functions, N_{basis} . In this section, we took a twice larger number of Monte Carlo sampling in the HF and TC calculations than that shown in the previous section (i.e., that used in other sections), to reduce the statistical error.

Figure 1 presents the total energy plotted against the inverse of the number of basis functions, N_{basis}^{-1} , (a) for the HF method and (b) for the TC method (E_{TC}) using the $S = S_{\text{minimum}} = \{(1, 0, 0)\}$ Jastrow function in Eq. (25) with $a = 1.5$ Bohr. Based on these plots, we determined to set $N_{\text{basis}} = 50$ from the next section both for the HF and (Bi)TC calculations, by which an expected basis-set error is sufficiently small (~ 0.1 mHt). We note that our Hartree-Fock energy of a helium atom with $N_{\text{basis}}^{-1} \rightarrow 0$ (i.e. $N_{\text{basis}} \rightarrow \infty$) is consistent with the complete-basis-set limit reported in an old literature (-2.861679995612 Ht.) [59]. A small difference mainly comes from the statistical error in Monte Carlo sampling and possibly also from the number of spatial meshes in our calculation, while it is not the scope of our study to see the convergence at the level of 0.1 mHt. We do not show the BiTC result since it shows the same trend as the TC result.

C. Total energy and orbital energy

1. Total energy

First, we compare the calculated total energies under several conditions in Fig. 2. For HF+VMC calculation, we evaluated the total energy, Eq. (9), by VMC, which is denoted as $E_{\text{VMC}}^{\text{HF+VMC}}$ in Fig. 2. On the other hand, for TC+VMC calculation, we have three ways to estimate the total energy. The total energy, Eq. (9), evalu-

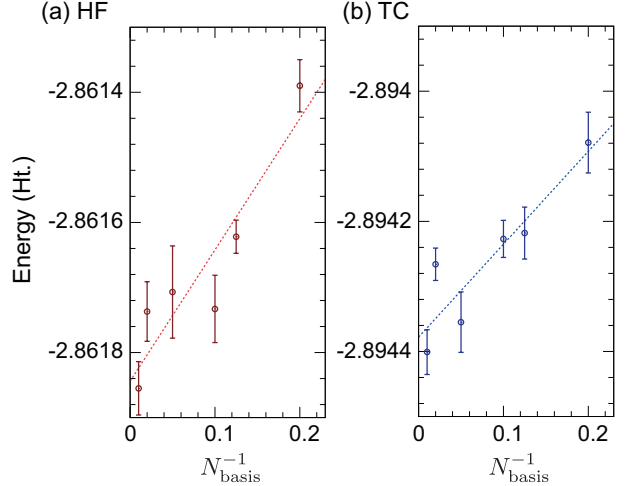


FIG. 1: Total energy plotted against the inverse of the number of basis functions, N_{basis}^{-1} , (a) for the HF method and (b) for the TC method (E_{TC}) using the $S = S_{\text{minimum}} = \{(1, 0, 0)\}$ Jastrow function in Eq. (25) with $a = 1.5$ Bohr. Lines are guides for eyes.

ated by VMC is denoted as $E_{\text{VMC}}^{\text{TC+VMC}}$, and those evaluated by Eqs. (10) and (11) are denoted as $E_{\text{TC}}^{\text{TC+VMC}}$ and $E_{\text{BiTC}}^{\text{TC+VMC}}$, respectively. These different estimates of the total energy coincide when the many-body wave function is the exact eigenstate. The calculated total energies are also listed in Table I, where $a = 1.5$ Bohr for the S_{ee} and S_{een} Jastrow functions are chosen as representative cases.

In Fig. 2(a), it is shown that the TC orbital optimization successfully improves a quality of the many-body wave function, because $E_{\text{VMC}}^{\text{TC+VMC}}$ is lower than $E_{\text{VMC}}^{\text{HF+VMC}}$. This improvement is also found for the S_{ee} Jastrow function as shown in Fig. 2(b)(d). Because higher-order polynomial terms are included for the S_{ee} Jastrow function, the total energy less depends on the Jastrow parameter a (shown as the horizontal axis) in Fig. 2(b)(d) unlike in Fig. 2(a). It is also noteworthy that the best a parameter in Fig. 2(a) provides a similar E_{VMC} to that in Fig. 2(b)(d), which might be due to a simplicity of the Jastrow function for a helium atom. When using the S_{een} Jastrow function, $E_{\text{VMC}}^{\text{TC+VMC}}$ and $E_{\text{VMC}}^{\text{HF+VMC}}$ are very similar as shown in Fig. 2(c)(e). This might not be the case for other atoms where nodal one-body wave functions are included in the Slater determinant, because a nodal structure cannot be represented with the Jastrow factor, which is an important future issue.

While E_{VMC} is variational, $E_{\text{(Bi)TC}}$ is not so because of the non-Hermiticity of the TC Hamiltonian. Related to this feature, although evaluated for the same many-body wave function, $E_{\text{VMC}}^{\text{TC+VMC}}$, $E_{\text{TC}}^{\text{TC+VMC}}$, and $E_{\text{BiTC}}^{\text{TC+VMC}}$ are largely different in Fig. 2(a). This discrepancy becomes smaller by improving the Jastrow factor, as shown in Fig. 2(b)–(e). In total, $E_{\text{TC}}^{\text{TC+VMC}}$ tends to be too low,

i.e. overcorrelated, for low-quality Jastrow factors, but it is somewhat alleviated for $E_{\text{BiTC}}^{\text{TC+VMC}}$ (also see Table I). It is likely because the left (bra) orbital in the BiTC method tends to delocalize compared with the HF orbital, which is the opposite trend to the right (ket) orbital in the (Bi)TC method, as we shall see in Sec. V D 2. The TC total energy is overcorrelated also for solid-state calculation [31].

One important problem we found is a high sensitivity of $E_{(\text{Bi})\text{TC}}^{\text{TC+VMC}}$ to the Jastrow parameters. This is seen, e.g., from a large variation of $E_{(\text{Bi})\text{TC}}^{\text{TC+VMC}}$ for $2 \leq a \leq 3$ Bohr in Fig. 2(a), while $E_{\text{VMC}}^{\text{TC+VMC}}$ evaluated using the same right one-electron orbitals is almost unchanged against the a parameter. We speculate that such high sensitivity is to some extent relevant to the non-Hermiticity of \mathcal{H}_{TC} discussed above that breaks the variational principle and then the variation of $E_{(\text{Bi})\text{TC}}^{\text{TC+VMC}}$ is not restricted by the exact total energy. This might be related to the sizable difference of $E_{(\text{Bi})\text{TC}}^{\text{TC+VMC}}$ between the energy- and variance-minimized calculations for the S_{ee} Jastrow function as shown in Fig. 2(b)(d), where E_{VMC} is not so different between the energy- and variance-minimization. Such a difference between the energy- and variance-minimization is not significant when using a better S_{seen} Jastrow function as shown in Fig. 2(c)(e). The energy curves of $E_{(\text{Bi})\text{TC}}^{\text{TC+VMC}}$ in Fig. 2(c)(e) are not very smooth against the a parameter, because of the high-sensitivity of those energies to the Jastrow parameters $c_{ijk}^{\sigma_1\sigma_2}$, which makes a difficulty in achieving the self-consistency for the TC+VMC calculations. One possible way to evade this issue is non-self-consistent approach where the Jastrow parameters optimized for the HF orbitals are used in the TC calculation, as adopted in Ref. [44]. We shall discuss the effect of the iterative TC and VMC calculations (to say, the self-consistency in the TC+VMC calculation) in Sec. V E.

We here make a few comments on the consistency with the previous study by Umezawa *et al.* [14]. They calculated the total energies, $E_{\text{VMC}}^{\text{HF+VMC}}$, $E_{\text{VMC}}^{\text{TC+VMC}}$, and $E_{\text{TC}}^{\text{TC+VMC}}$, by using S_{minimum} Jastrow function with the best a parameter ($a = 1.92$ Bohr). The ratio of the retrieved correlation energies were reported as 61%, 90%, and 77% for $E_{\text{VMC}}^{\text{HF+VMC}}$, $E_{\text{VMC}}^{\text{TC+VMC}}$, and $E_{\text{TC}}^{\text{TC+VMC}}$, respectively. We calculated these values using the same Jastrow function, and obtained 53.5%, 90.3%, and 106.8%, respectively. They are roughly consistent except for $E_{\text{TC}}^{\text{TC+VMC}}$. One possible reason for the difference of $E_{\text{TC}}^{\text{TC+VMC}}$ is a basis-set error for the one-electron orbitals in the previous study. Because of the coincidence of E_{VMC} and E_{TC} in the S_{seen} Jastrow function as shown in Fig. 2(c)(e), we consider that $E_{\text{TC}}^{\text{TC+VMC}}$ calculated by us using a larger number of basis functions is reliable. Another important difference between Umezawa and us is that the fact that σ_{TC}^2 is minimized in their calculation, as mentioned in Sec. IV. Regarding this point, the best a parameter for S_{minimum} in Ref. [14], $a = 1.92$

Bohr, seems to be consistent with our calculation (see Fig. 2(a)), which suggests that σ_{TC}^2 minimization also works well as a guiding principle for Jastrow optimization.

2. Orbital energy

Because the (Bi)TC method can be regarded as a single-Slater-determinant (HF) approximation for the similarity-transformed Hamiltonian, we can naturally obtain the orbital energies in Eq. (8), and $\text{Re}[\epsilon_{ii}]$ satisfies the Koopmans' theorem as proved in Ref. [14]. In this section, we investigate the accuracy of the orbital energy. From this section, we consider the S_{ee} and S_{seen} Jastrow functions using $a = 1.5$ Bohr as representative cases, because of a small a -dependence of the total energy in Fig. 2(b)–(e).

Table II presents the calculated ionization potential (IP) estimated from the $1s$ orbital energy. We can see that IP estimated from HF is the closest to the exact value, and TC and BiTC tend to overestimate it. The reason can be understood by the following reason. It is well known that, in the HF method, two errors of IP is partially canceled out: one is a lack of the correlation effects and the other one is a lack of the orbital relaxation that actually takes place when an electron is removed from an atom. The former error gives a high total energy of He, and thus results in underestimation of IP. On the other hand, the latter overestimate the total energy of He^+ , which results in overestimation of IP. While IP is relatively accurate for HF by such an error cancelation, the former error is expected to be small in (Bi)TC because of the inclusion of the electron correlation effects. Thus, the overestimation of IP is expected in (Bi)TC because of the lack of the orbital relaxation in He^+ . Note that this is not the failure of the (Bi)TC method itself, but rather due to the limitation of the Koopmans' theorem. It is an important future issue to see how the situation changes for larger atoms where the relaxation effect is expected to become smaller. The ionization potentials of 0.9180 Ht. for HF and 0.9179 Ht. for TC using $a = 1.92$ Bohr for S_{minimum} were reported in Ref. [14], the former of which is consistent with ours while we obtained 0.9290 Ht. for TC using the same Jastrow factor. A discrepancy of IP for TC is likely relevant to the difference in E_{TC} as discussed in the previous section, the origin of which might be the basis-set error in the previous study.

D. Optimized many-body wave functions

1. Optimized Jastrow functions

Figure 3 presents the optimized Jastrow factor, $F(x_1, x_2) = \exp(-u(x_1, x_2))$ for several conditions that we have discussed in the previous sections. The position of one electron, \mathbf{r}_2 , is fixed at $\mathbf{r}_2 = (1.65, 0, 0)$ (Bohr)

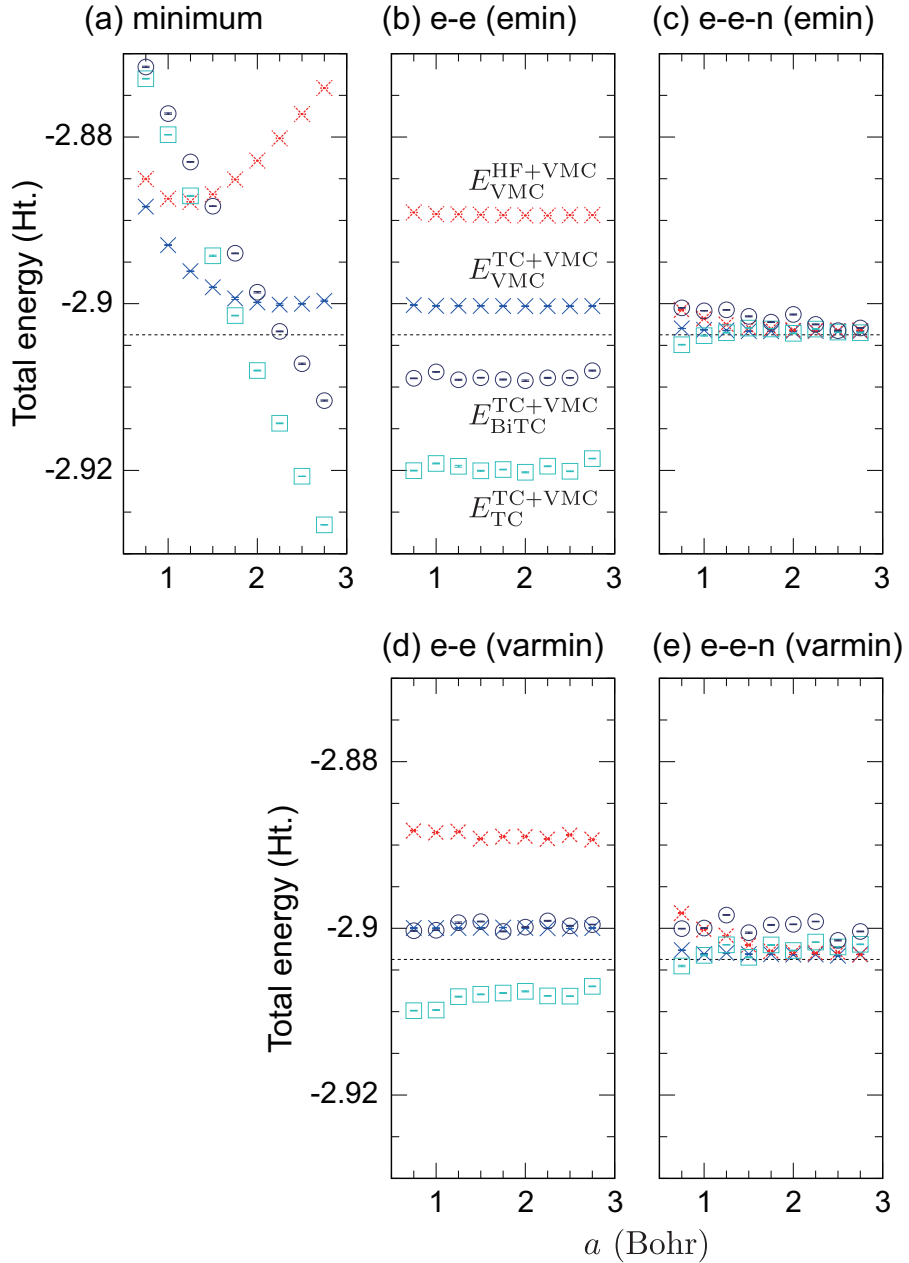


FIG. 2: Calculated total energies using the Jastrow functions with (a) $S = S_{\text{minimum}}$, (b)(d) $S = S_{\text{ee}}$, (c)(e) $S = S_{\text{een}}$, respectively. For panels (b)(c), energy minimization was adopted in VMC calculation. For panels (d)(e), variance minimization was adopted. The broken lines show the exact total energy ($E_{\text{exact}} = -2.90372$ Ht.) estimated in Ref. 60.

as shown in Fig. 3(a). In addition, the z coordinate of $\mathbf{r}_1 = (x_1, y_1, z_1)$ is fixed at 0, i.e., $z_1 = 0$, in this plot. The spin coordinates of two electrons are assumed to be antiparallel ($\sigma_1 = -\sigma_2$).

In Figs. 3(a)(c), contour lines are concentric circles because the Jastrow factor only has a $|\mathbf{r}_1 - \mathbf{r}_2|$ dependence. A small weight of the Jastrow factor near $\mathbf{r}_1 \sim \mathbf{r}_2$ represents that electrons avoid each other by strong Coulomb repulsion. By including the S_{een} Jastrow terms, in Figs. 3(b)(d), the Jastrow function can exhibit more complex behavior. Here, a weight of the Jastrow fac-

tor near the nucleus increases to some extent compared with Figs. 3(a)(c), which is a natural consequence of the electron-nucleus attractive interaction. In other words, the electron-electron-nucleus terms in the Jastrow function alleviate the overscreening caused by the S_{ee} Jastrow function, which does not take into account the position of the nucleus. We can see this trend also in Fig. 4, where the same plot constrained on the $y_1 = z_1 = 0$ line is shown. It is interesting that the trend mentioned above is more conspicuous for the Jastrow factors obtained by the energy minimization than for those obtained by the

TABLE I: Total energy (Ht.) and the ratio of the correlation energy retrieved (%) for each method. For evaluating the latter quantity, the HF energy calculated by us using $N_{\text{basis}} = 50$ ($E_{\text{HF}} = -2.8617(3)$ Ht.) and the exact total energy ($E_{\text{exact}} = -2.90372$ Ht.) estimated in Ref. 60 were used. For all data except those taken from Ref. [14], $a = 1.5$ Bohr was used in the Jastrow factor. For data taken from Ref. [14], $a = 1.92$ Bohr was used as the best value obtained by the variance (σ_{TC}^2) minimization. The statistical error for our calculation results are not shown in this table because it is much less than the expected basis-set error ~ 0.1 mHt.

VMC type	Method	Jastrow type	E_{VMC}	(%)	E_{TC}	(%)	E_{BiTC}	(%)	Ref.
emin	HF+VMC	S_{ee}	-2.8893	65.7	-	-	-	-	-
		S_{seen}	-2.9029	98.0	-	-	-	-	-
	TC+VMC	S_{ee}	-2.9003	91.7	-2.9201	138.8	-2.9089	112.3	-
		S_{seen}	-2.9033	99.0	-2.9029	98.1	-2.9015	94.8	-
varmin	HF+VMC	S_{ee}	-2.8893	65.6	-	-	-	-	-
		S_{seen}	-2.9012	93.9	-	-	-	-	-
	TC+VMC	S_{ee}	-2.8999	91.0	-2.9079	110.0	-2.8992	89.2	-
		S_{seen}	-2.9031	98.5	-2.9035	99.4	-2.9005	92.4	-
(σ_{TC}^2)	HF+VMC	S_{minimum}	-2.8873(8)	61	-	-	-	-	[14]
	TC+VMC	S_{minimum}	-2.8997(4)	90	-2.8942	77	-	-	[14]

TABLE II: Ionization potential (IP) (Ht.) estimated from the $1s$ orbital energy. The exact IP is determined from a difference between the exact total energy of helium atom, $E_{\text{exact}} = -2.90372$ Ht. estimated in Ref. 60, and the exact total energy of He^+ , -2.0 Ht. For all data except those taken from Ref. [14], $a = 1.5$ Bohr was used in the Jastrow factor. For data taken from Ref. [14], $a = 1.92$ Bohr was used as the best value obtained by the variance (σ_{TC}^2) minimization. The statistical error for our calculation results are not shown in this table because it is much less than the expected basis-set error ~ 0.1 mHt.

VMC type	Method	Jastrow type	IP	Ref.
-	HF	-	0.9180	-
-	HF	-	0.9180	[14]
emin	TC	S_{ee}	0.9380	-
		S_{seen}	0.9432	-
	BiTC	S_{ee}	0.9596	-
		S_{seen}	0.9552	-
varmin	TC	S_{ee}	0.9301	-
		S_{seen}	0.9368	-
	BiTC	S_{ee}	0.9507	-
		S_{seen}	0.9538	-
varmin	TC	S_{minimum}	0.9179	[14]
	(σ_{TC}^2)	-	-	
-	Exact	-	0.90372	[60]

variance minimization. Note that, in Figs. 3 and 4, a constant multiplication of the Jastrow factor is meaningless because this degree of freedom is absorbed in the normalization condition of the many-body wave function. In our definition, the one-electron orbitals in the Slater determinant are only normalized. Even though, the VMC total energy, $\langle \Phi F | \mathcal{H} | F \Phi \rangle / \langle F \Phi | F \Phi \rangle$ is appropriately defined. In the (Bi)TC method, not F but $F^{-1} \mathcal{H} F$ is used in equations, where such a constant multiplication does not play any role.

To see the role of the Jastrow factor in more detail, in Fig. 5, we show the TC effective potential of the electron

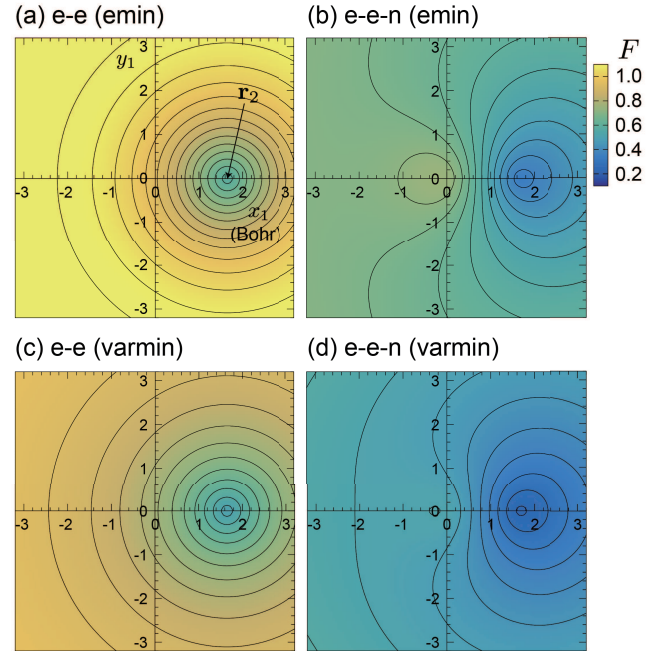


FIG. 3: Optimized Jastrow factor $F(x_1, x_2) = \exp(-u(x_1, x_2))$, with constraints of $z_1 = 0$, $\mathbf{r}_2 = (1.65, 0, 0)$ (Bohr), and $\sigma_1 = -\sigma_2$ (see the main text). For panels (a)(b), energy minimization was adopted in VMC calculation. For panels (c)(d), variance minimization was adopted. The S_{ee} and S_{seen} Jastrow functions were used for panels (a)(c) and (b)(d), respectively. For all the panels, $a = 1.5$ Bohr was used.

at $x_1 = (\mathbf{r}_1, \sigma_1)$ defined as follows:

$$V_{\text{eff}}(x_1, x_2) \equiv -\frac{2}{|\mathbf{r}_1|} + \frac{1}{|\mathbf{r}_1 - \mathbf{r}_2|} + \frac{\nabla_1^2 u(x_1, x_2) + \nabla_2^2 u(x_1, x_2)}{2}, \quad (28)$$

where the first and second terms represent the electron-nucleus and electron-electron Coulomb potentials, respectively. Here we took a part of the TC effective in-

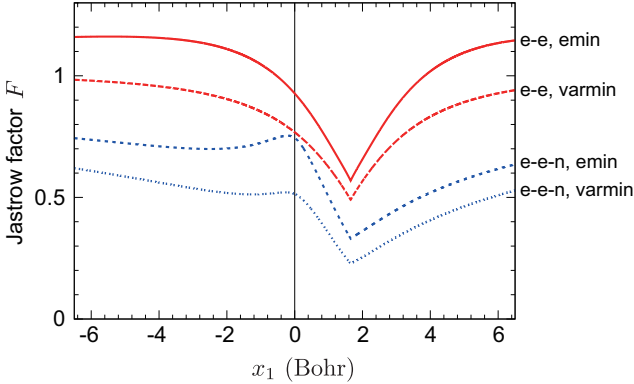


FIG. 4: The same plot as Fig. 3 on the $y_1 = z_1 = 0$ line. Each line represents the Jastrow factor F shown in Figs. 3(a)–(d).

teraction terms that describes the electron-electron cusp condition, to say, that exhibits a divergent behavior near the electron-electron coalescence point. Other effective potential terms have a relatively minor role near the electron-electron coalescence point since they do not exhibit such a divergent behavior, and are not shown here for simplicity. Details for plotting, such as the fixed \mathbf{r}_2 , are the same as those used for Fig. 3.

Comparing with Fig. 5(a), where the ‘bare’ potential (i.e. V_{eff} without $\nabla^2 u$ terms) is shown, we can clearly see, in Figs. 5(b)–(e), that the TC effective potential terms $\nabla^2 u$ successfully cancel out the divergence of the bare electron-electron Coulomb interaction at the electron-electron coalescence point. Under the weak effective electron-electron interaction, the mean-field (HF) approximation of the TC Hamiltonian is expected to work well. This is the way how the TC method takes into account the electron correlation effects. The same plot constrained on the $y_1 = z_1 = 0$ line is shown in Fig. 6.

In addition to the above-mentioned trend, we can also see that the effective potential for the S_{een} Jastrow function is a bit larger than that for the S_{ee} Jastrow function, and is rather close to the bare potential, near the nucleus (e.g. $|x_1| \leq 1$ Bohr). This means that the S_{een} Jastrow terms alleviate the overscreening near the nucleus by the S_{ee} Jastrow function, as we have seen in Figs. 3 and 4.

2. Optimized one-electron orbitals

Figure 7 presents the optimized one-electron orbitals of the $1s$ state. Here, the left orbital χ is shown for the BiTC method because a difference of ϕ between TC and BiTC is almost discernible. We can clearly see that the one-electron orbital is deformed by optimization in the (Bi)TC method. Overall, the right orbital ϕ is a bit localized compared with the HF orbital, while the left orbital χ is rather a bit delocalized. The reason why the right orbital ϕ is localized in the (Bi)TC method is as follows: the electron-electron interaction is screened by

the Jastrow factor and then an electron is allowed to become closer to the nucleus to get stabilized. It seems that the one-electron orbital is a bit over-localized for the S_{ee} Jastrow function, while it is somewhat weakened for the S_{een} Jastrow function, as is consistent with our observation discussed in the previous section. The opposite trend for localization between ϕ and χ originates from the fact that the left orbital can be regarded as the mean-field solution for $F\mathcal{H}F^{-1}$ rather than $\mathcal{H}_{\text{TC}} = F^{-1}\mathcal{H}F$, where the effect of the Jastrow factor is expected to be inverted.

E. Effect of the self-consistency between the Jastrow- and orbital-optimizations

Finally, we describe the effects of the self-consistent loop in TC+VMC, i.e., alternate optimization of the Jastrow parameters in VMC and one-electron orbitals in (Bi)TC. Table III summarizes the calculation results. Here, E_{VMC} was evaluated in the one-shot TC+VMC method by the following procedure: (i) perform the HF method to get the HF orbitals, (ii) perform the HF+VMC calculation to get the HF-optimized Jastrow factor, (iii) perform the TC method using the Jastrow parameters obtained in (ii), and (iv) evaluate E_{VMC} for the Jastrow parameters obtained in (ii) and the TC orbitals obtained in (iii). The alternative calculations of VMC and TC until the Jastrow parameters are not further optimized, which were done in the self-consistent TC+VMC calculations shown in the previous sections, were not performed here. In other words, the Jastrow parameters optimized for the HF orbitals were used for the one-shot TC+VMC calculations, as adopted in Ref. [44]. Note that the self-consistency for solving the one-body SCF equation, Eq. (8), in the HF or TC method is always satisfied.

We can see that one-shot TC+VMC to some extent improves a quality of the many-body wave function, i.e., lowers E_{VMC} , and so can be a good alternative way when one would like to reduce computational cost. On the other hand, it is also clear that the quality of the many-body wave function for one-shot TC+VMC is always inferior to that for self-consistent TC+VMC. One should take care of such a difference for each system. For a very simple system like our case, TC+VMC calculation using the S_{minimum} Jastrow function with the optimal a can also be a good alternative of that using the (self-consistently optimized) S_{ee} Jastrow function, because the former does not require a self-consistent optimization of the Jastrow parameters but offers the same accuracy as the latter as discussed in Sec. V C 1. Note that this strategy works well only for simple systems where the S_{minimum} Jastrow function well approximates the optimized one.

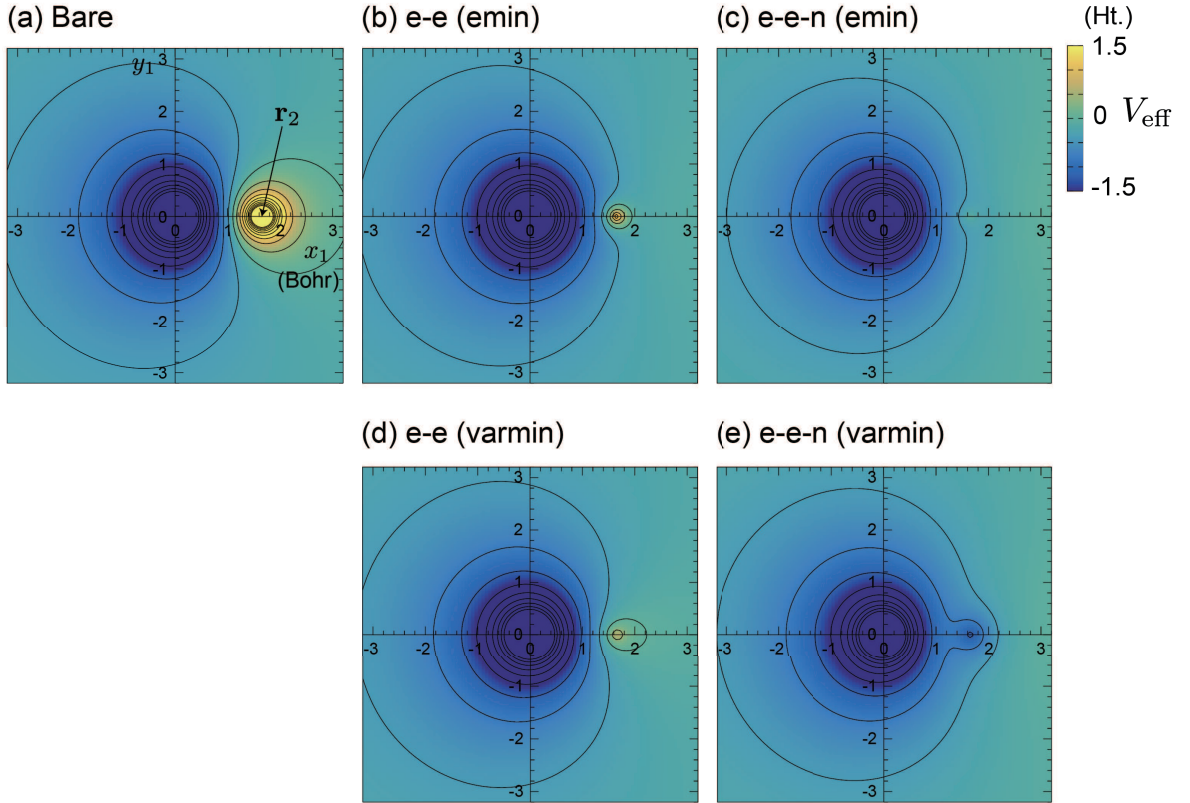


FIG. 5: TC effective potential $V_{\text{eff}}(x_1, x_2)$ as defined in Eq. (28), with constraints of $z_1 = 0$, $\mathbf{r}_2 = (1.65, 0, 0)$ (Bohr), and $\sigma_1 = -\sigma_2$ (see the main text). (a) The bare potential, to say, V_{eff} without $\nabla^2 u$ terms, is shown, instead of the TC effective potential. (b)–(e) The TC effective potential for several conditions, which are the same as those for Fig. 3(a)–(d). Contour lines are shown as guides for eyes.

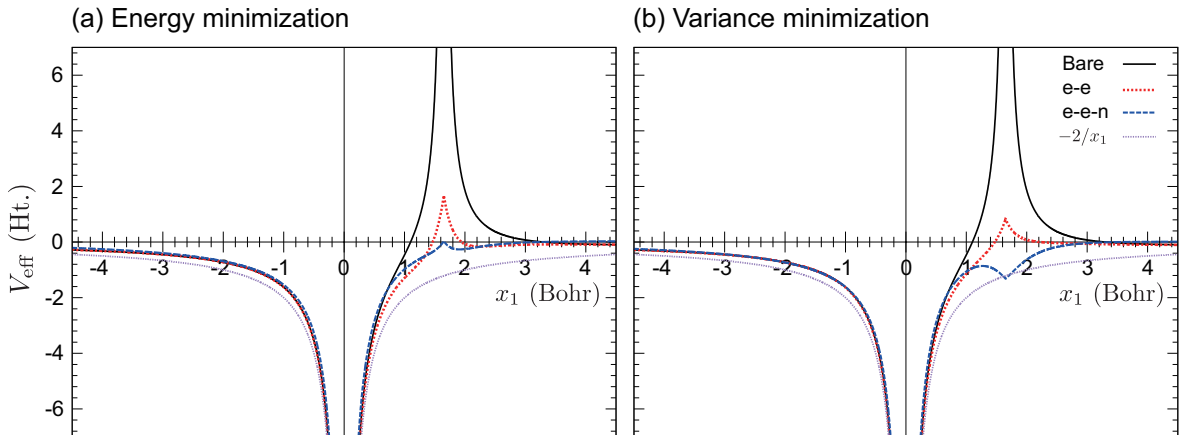


FIG. 6: The same plot as Fig. 5 on the $y_1 = z_1 = 0$ line. Panel (a) includes the results obtained by energy minimization in VMC, corresponding to Figs. 5(b)–(c), and panel (c) includes the results obtained by variance minimization in VMC, corresponding to Figs. 5(d)–(e). In both panels, $-2/x_1$, the Coulomb potential from the nucleus, is also shown as a guide for eyes.

VI. CONCLUSION

In this study, we have investigated a helium atom as a test case using the self-consistent TC+VMC method. We have found that the total energy is systematically improved by using better Jastrow functions, and the ex-

pectation value of the TC Hamiltonian, E_{TC} , goes closer to that of the original Hamiltonian, E_{VMC} , accordingly. The former quantity can be a good estimate of the total energy when one includes the electron-electron-nucleus terms into the Jastrow function. We have also seen that the orbital optimization in the TC method can be nat-

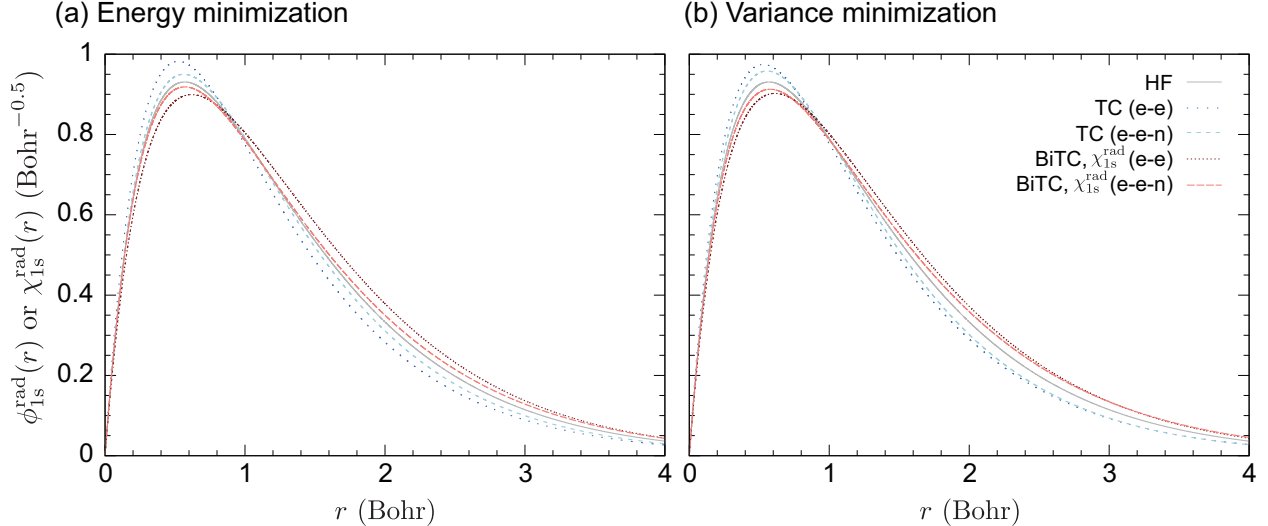


FIG. 7: The radial wave function for the 1s state. For the TC and BiTC orbitals, Jastrow functions were optimized by (a) energy minimization or (b) variance minimization. The left orbital χ is shown for the BiTC method. The right orbital ϕ for the BiTC method are not shown since a difference of ϕ between TC and BiTC is almost discernible.

TABLE III: Total energy (Ht.), the ratio of the correlation energy retrieved (%), and the ionization potential (IP) (Ht.) estimated from the 1s orbital energy for each method. Details are the same as those for Tables I and II. Calculated results for HF+VMC and self-consistent TC+VMC are taken from Tables I and II. IP was evaluated in HF or TC calculations.

VMC type	Jastrow type	Method	E_{VMC}	(%)	IP
emin	S_{ee}	HF+VMC	-2.8893	65.7	0.9180
		TC+VMC (one-shot)	-2.8967	83.2	0.9241
		TC+VMC (self-consistent)	-2.9003	91.7	0.9380
seen	S_{een}	HF+VMC	-2.9029	98.0	0.9180
		TC+VMC (one-shot)	-2.9030	98.4	0.9518
		TC+VMC (self-consistent)	-2.9033	99.0	0.9432
varmin	S_{ee}	HF+VMC	-2.8893	65.6	0.9180
		TC+VMC (one-shot)	-2.8967	83.4	0.9244
		TC+VMC (self-consistent)	-2.8999	91.0	0.9301
	S_{een}	HF+VMC	-2.9012	93.9	0.9180
		TC+VMC (one-shot)	-2.9024	96.9	0.9394
		TC+VMC (self-consistent)	-2.9031	98.5	0.9368

urally understood by considering the role of the Jastrow factor and the effective potential induced by it. One can partially receive the benefit of the orbital optimization even by one-shot TC+VMC, where the Jastrow parameters are optimized at the HF+VMC level, while a quality of the many-body wave function is inferior to that for self-consistent TC+VMC. Our study provides important knowledge for optimizing many-body wave function including the Jastrow correlation factor, which would be of great help for development of highly accurate electronic structure calculation.

ACKNOWLEDGMENTS

This study was supported by Grant-in-Aid for young scientists (Grant Number JP18K13470) from the Japan

Society for the Promotion of Science, Japan. We thank Prof. Shinji Tsuneyuki for fruitful discussion.

Appendix A: Orthonormality of the basis set $f_n^{l_i}$

Using a formula

$$\int_0^\infty x^a e^{-x} L_m^{(a)}(x) L_n^{(a)}(x) dx = \frac{(n+a)!}{n!} \delta_{m,n}, \quad (29)$$

one can verify that $f_n^{l_i}$ is orthonormalized as follows:

$$\int_0^\infty f_n^{l_i}(r) f_m^{l_i}(r) dr = \sqrt{\frac{m!n!}{(m+2l_i+2)!(n+2l_i+2)!}} \int_0^\infty (2\alpha r_i)^{2l_i+2} e^{-2\alpha r} L_m^{2l_i+2}(2\alpha r) L_n^{2l_i+2}(2\alpha r) d(2\alpha r) \quad (30)$$

$$= \sqrt{\frac{m!n!}{(m+2l_i+2)!(n+2l_i+2)!}} \frac{(n+2l_i+2)!}{n!} \delta_{m,n} \quad (31)$$

$$= \delta_{m,n}. \quad (32)$$

Appendix B: Calculation of Eq. (17)

For simplicity, we omit the normalization constant in $f_n^{l_i}$ here. To say, we evaluate the integral for $\tilde{f}_n^{l_i} =$

$r^{l_i+1} L_n^{(2l_i+2)}(2\alpha r) e^{-\alpha r}$ instead of that for $f_n^{l_i}$. We only consider the $m \geq n$ case, the other case of which ($m < n$) is readily derived by Hermiticity. The first term in Eq. (17) is written as follows:

$$-\frac{1}{2} \int_0^\infty dr \tilde{f}_m^{l_i}(r) \frac{d^2}{dr^2} \tilde{f}_n^{l_i}(r) \quad (33)$$

$$= -\frac{1}{2} \int_0^\infty dr \tilde{f}_m^{l_i}(r) \left[\left(\frac{d^2}{dr^2} r^{l_i+1} \right) L_n^{(2l_i+2)}(2\alpha r) e^{-\alpha r} + r^{l_i+1} \left(\frac{d^2}{dr^2} L_n^{(2l_i+2)}(2\alpha r) \right) e^{-\alpha r} \right. \quad (34)$$

$$\begin{aligned} &+ r^{l_i+1} L_n^{(2l_i+2)}(2\alpha r) \left(\frac{d^2}{dr^2} e^{-\alpha r} \right) + 2 \left(\frac{d}{dr} r^{l_i+1} \right) \left(\frac{d}{dr} L_n^{(2l_i+2)}(2\alpha r) \right) e^{-\alpha r} \\ &+ 2 \left(\frac{d}{dr} r^{l_i+1} \right) L_n^{(2l_i+2)}(2\alpha r) \left(\frac{d}{dr} e^{-\alpha r} \right) + 2r^{l_i+1} \left(\frac{d}{dr} L_n^{(2l_i+2)}(2\alpha r) \right) \left(\frac{d}{dr} e^{-\alpha r} \right) \left. \right]. \end{aligned}$$

The first term in Eq. (34) is rewritten as $\int_0^\infty dr \tilde{f}_m^{l_i}(r) \frac{-l_i(l_i+1)}{2r^2} \tilde{f}_n^{l_i}(r)$, which cancels out the second term in Eq. (17). The second and sixth terms in Eq. (34) are zero because of the orthonormalization condition (Eq. (29)) and the fact that any l -th polynomial

can be represented as linear combination of $L_i^{(a)}$ with $i \leq l$. The third term in Eq. (34) gives the first term in Eq. (18). For calculating the fourth term, we note

$$\left(\frac{d}{dr} r^{l_i+1} \right) \left(\frac{d}{dr} L_n^{(2l_i+2)}(2\alpha r) \right) = r^{l_i+1} \times ((n-2)-\text{th order polynomial}) - 2\alpha(l_i+1)r^{l_i} \binom{n+2l_i+2}{n-1} \quad (35)$$

$$= r^{l_i+1} \times ((n-1)-\text{th order polynomial}) - 2\alpha(l_i+1)r^{l_i} \frac{n}{2l_i+3} L_n^{(2l_i+2)}(2\alpha r), \quad (36)$$

which is derived using the coefficients of the zeroth- and first-order terms in the associated Laguerre polynomial. The first term in Eq. (36) makes no contribution to Eq. (34) because of the orthogonality of the associated Laguerre polynomials and $m > n-1$. The second term in Eq. (36) yields

$$2\alpha \frac{(l_i+1)n}{2l_i+3} \int_0^\infty dr \tilde{f}_m^{l_i}(r) \frac{1}{r} \tilde{f}_n^{l_i}(r). \quad (37)$$

Note that n in the coefficient of this integral should be

replaced with $\min(m, n)$ when one considers not only the $m \geq n$ case but also $m < n$. The fifth term in Eq. (34) gives $\int_0^\infty dr \tilde{f}_m^{l_i}(r) \frac{\alpha(l_i+1)}{r} \tilde{f}_n^{l_i}(r)$. By summing up all of them, we can obtain Eq. (18) (see also Appendix in [49]).

Appendix C: Derivation of Eq. (22)

Spherical harmonics is defined as follows:

$$Y_{l,m}(\Omega) = (-1)^{\frac{m+|m|}{2}} \sqrt{\frac{2l+1}{4\pi} \frac{(l-|m|)!}{(l+|m|)!}} P_l^{|m|}(\cos\theta) e^{im\varphi}, \quad (38)$$

where $P_\nu^\mu(t)$ are associated Legendre polynomials satisfying the following formula,

$$\sin^2 \theta \frac{d}{dt} P_\nu^\mu(t) = \sin \theta P_\nu^{\mu+1}(t) - \mu \cos \theta P_\nu^\mu(t). \quad (39)$$

By using these equations, we can immediately derive Eq. (22).

Appendix D: Derivatives of the Jastrow function used in this study

While the analytical derivative of the Jastrow function, Eq. (25), is straight-forward, we present mathematical expressions for reference, which can be helpful in implementing the TC method. A simple calculation yields

$$\nabla_1 u(x_1, x_2) = \sum_{(i,j,k) \in S} c_{ijk}^{\sigma_1 \sigma_2} \bar{r}_{12}^{i-1} \bar{r}_1^{j-1} \bar{r}_2^k \times \left(\frac{\mathbf{r}_{12}}{r_{12}} \frac{ia_{12}}{(r_{12} - a_{12})^2} \bar{r}_1 + \frac{\mathbf{r}_1}{r_1} \frac{ja}{(r_1 - a)^2} \bar{r}_{12} \right), \quad (40)$$

and

$$\nabla_1^2 u(x_1, x_2) = \sum_{(i,j,k) \in S} c_{ijk}^{\sigma_1 \sigma_2} \bar{r}_{12}^{i-2} \bar{r}_1^{j-2} \bar{r}_2^k \times \left(\frac{(i+1)ia_{12}^2}{(r_{12} + a_{12})^4} \bar{r}_1^2 + \frac{(j+1)ja^2}{(r_1 + a)^4} \bar{r}_{12}^2 \right. \quad (41)$$

$$\left. + \frac{\mathbf{r}_{12} \cdot \mathbf{r}_1}{r_{12} r_1} \frac{2ija_{12}a}{(r_{12} + a_{12})^2 (r_1 + a)^2} \right), \quad (42)$$

by which we can readily write down the TC effective potentials represented with ∇u and $\nabla^2 u$. We note that a sign of the coefficients $c_{ijk}^{\sigma_1 \sigma_2}$ should be reversed when one defines the Jastrow factor as $F = \exp(\sum_{i,j(i \neq j)}^N u(x_i, x_j))$, unlike our notation shown in Eq. (2).

DATA AVAILABILITY

The data that support the findings of this study are available from the corresponding author upon reasonable request.

[1] T. Kato, Commun. Pure Appl. Math. **10**, 151 (1957).
[2] R. T. Pack and W. B. Brown, J. Chem. Phys. **45**, 556 (1966).
[3] E. A. Hylleraas, Z. Phys. **48**, 469 (1928).
[4] E. A. Hylleraas, Z. Phys. **54**, 347 (1929).
[5] E. A. Hylleraas, Z. Phys. **65**, 209 (1930).
[6] W. Kutzelnigg, Theor. Chim. Acta **68**, 445 (1985).
[7] S. Ten-no, Chem. Phys. Lett. **398**, 56 (2004).
[8] R. J. Needs, M. D. Towler, N. D. Drummond, and P. López Ríos, J. Phys.: Condens. Matter **22**, 023201 (2009).
[9] W. M. C. Foulkes, L. Mitas, R. J. Needs, and G. Rajagopal, Rev. Mod. Phys. **73**, 33 (2001).
[10] S. F. Boys and N. C. Handy, Proc. R. Soc. London Ser. A **309**, 209 (1969); *ibid.* **310**, 43 (1969); *ibid.* **310**, 63 (1969); *ibid.* **311**, 309 (1969).
[11] N. C. Handy, Mol. Phys. **21**, 817 (1971).
[12] S. Ten-no, Chem. Phys. Lett. **330**, 169 (2000); *ibid.* 175 (2000).
[13] O. Hino, Y. Tanimura, S. Ten-no, J. Chem. Phys. **115**, 7865 (2001).
[14] N. Umezawa and S. Tsuneyuki, J. Chem. Phys. **119**, 10015 (2003).
[15] O. Hino, Y. Tanimura, S. Ten-no, Chem. Phys. Lett. **353**, 317 (2002).
[16] N. Umezawa and S. Tsuneyuki, J. Chem. Phys. **121**, 7070 (2004).
[17] H. Luo, J. Chem. Phys. **133**, 154109 (2010).
[18] H. Luo, J. Chem. Phys. **135**, 024109 (2011).
[19] E. Giner, J. Chem. Phys. **154**, 084119 (2021).
[20] T. Yanai and T. Shiozaki, J. Chem. Phys. **136**, 084107 (2012).
[21] M. Motta, T. P. Gujarati, J. E. Rice, A. Kumar, C. Maseran, J. A. Latone, E. Lee, E. F. Valeev, and T. Y. Takeshita, Phys. Chem. Chem. Phys. **22**, 24270 (2020).
[22] S. Sharma, T. Yanai, G. H. Booth, C. J. Umrigar, and G. K.-L. Chan, J. Chem. Phys. **140**, 104112 (2014).
[23] J. A. F. Kersten, G. H. Booth, and A. Alavi, J. Chem. Phys. **145**, 054117 (2016).
[24] S. McArdle and D. P. Tew, arXiv:2006.11181.
[25] R. Sakuma and S. Tsuneyuki, J. Phys. Soc. Jpn. **75**, 103705 (2006).
[26] M. Ochi, K. Sodeyama, R. Sakuma, and S. Tsuneyuki, J. Chem. Phys. **136**, 094108 (2012).
[27] M. Ochi, K. Sodeyama, and S. Tsuneyuki, J. Chem. Phys. **140**, 074112 (2014).
[28] M. Ochi, Y. Yamamoto, R. Arita, and S. Tsuneyuki, J. Chem. Phys. **144**, 104109 (2016).
[29] M. Ochi, R. Arita, and S. Tsuneyuki, Phys. Rev. Lett. **118**, 026402 (2017).
[30] M. Ochi and S. Tsuneyuki, J. Chem. Theory Comput. **10**, 4098 (2014).
[31] M. Ochi and S. Tsuneyuki, Chem. Phys. Lett. **621**, 177 (2015).

[32] S. Tsuneyuki, *Prog. Theor. Phys. Suppl.* **176**, 134 (2008).

[33] W. Dobrautz, H. Luo, and A. Alavi, *Phys. Rev. B* **99**, 075119 (2019).

[34] A. Bardi and M. Reiher, *J. Chem. Phys.* **153**, 164115 (2020).

[35] J. M. Wahlen-Strothman, C. A. Jiménez-Hoyos, T. M. Henderson, and G. E. Scuseria, *Phys. Rev. B* **91**, 041114(R) (2015).

[36] E. A. G. Armour, *J. Phys. C: Solid State Phys.* **13**, 343 (1980).

[37] N. Umezawa and S. Tsuneyuki, *Phys. Rev. B* **69**, 165102 (2004).

[38] H. Luo, *J. Chem. Phys.* **136**, 224111 (2012).

[39] H. Luo and A. Alavi, *J. Chem. Theory. Comput.* **14**, 1403 (2018).

[40] P. Jeszenszki, H. Luo, A. Alavi, and J. Brand, *Phys. Rev. A* **98**, 053627 (2018).

[41] P. Jeszenszki, U. Ebling, H. Luo, A. Alavi, and J. Brand, *Phys. Rev. Res.* **2**, 043270 (2020).

[42] R. Prasad, N. Umezawa, D. Domin, R. Salomon-Ferrer, and W. A. Lester, Jr., *J. Chem. Phys.* **126**, 164109 (2007).

[43] H. Luo, W. Hackbusch, and H.-J. Flad, *Mol. Phys.* **108**, 425 (2010).

[44] A. J. Cohen, H. Luo, K. Guther, W. Dobrautz, D. P. Tew, and A. Alavi, *J. Chem. Phys.* **151**, 061101 (2019).

[45] J. Toulouse and C. J. Umrigar, *J. Chem. Phys.* **126**, 084102 (2007).

[46] J. Toulouse and C. J. Umrigar, *J. Chem. Phys.* **128**, 174101 (2008).

[47] D. Bohm and D. Pines, *Phys. Rev.* **92**, 609 (1953).

[48] S. Ten-no, *J. Chem. Phys.* **121**, 117 (2004).

[49] S. Hagstrom and H. Shull, *J. Chem. Phys.* **30**, 1314 (1959).

[50] Y. Hatano and S. Yamamoto, *J. Comput. Chem. Jpn. Int. Ed.* **2**, 2016-0003 (2016).

[51] The asymptotic behavior of the Hartree-Fock orbitals is investigated in old literature [52], and the same discussion holds for the (Bi)TC method. This fact originates from the exchange terms in the SCF equation, which brings $e^{-\sqrt{-2\epsilon_{HO}}r}$ asymptotic behavior for $r \rightarrow \infty$ (to say, the slowest decay among the occupied orbitals) to all the orbitals.

[52] N. C. Handy, M. T. Marron, and H. J. Silverstone, *Phys. Rev.* **180**, 45 (1969).

[53] When ϵ_{HO} happens to be positive in some SCF loop, we instead substituted some negative value such as $\epsilon_{\max} = -0.05$ Ry for $\alpha = \sqrt{-2\epsilon_{\max}}$ to keep the decaying behavior of the basis functions in the $r \rightarrow \infty$ limit. Of course, this should not happen in the final SCF loop.

[54] For the BiTC method, the operator acting on the right orbital ϕ in the left-hand side of the SCF equation is Hermitian conjugate of that for the left orbital χ . Thus, right and left orbitals are simultaneously obtained as the right and left eigenstates by diagonalizing the common matrix.

[55] Because of the non-Hermitian character of the similarity-transformed Hamiltonian, the eigenstates of the TC-SCF equation is not orthogonalized. Thus, actual calculation is proceeded as follows. First, we diagonalize the TC-SCF matrix and get its eigenstates. Next, we perform Gram-Schmidt orthonormalization of the orbitals to satisfy the orthogonality. Note that the orbitals with different (l_i, m_i, σ_i) are orthogonal even when the non-Hermiticity takes place, and hence this orthogonalization is performed within the same (l_i, m_i, σ_i) . These orthonormalized orbitals are the TC one-electron orbitals shown in this paper. Because the Gram-Schmidt orthonormalization (i.e. linear combination within the occupied orbitals) does not change the Slater determinant except a constant factor, this procedure does not change the many-body wave function. By using the orthonormalized orbitals, we can derived the TC-SCF equation, Eq.(8). The detail of this procedure was explained in Ref. [14]. For the BiTC method, the biorthogonal condition is imposed instead of the orthogonal condition, and so this issue does not take place.

[56] K. E. Schmidt and J. W. Moskowitz, *J. Chem. Phys.* **93**, 4172 (1990).

[57] C. Filippi and C. J. Umrigar, *J. Chem. Phys.* **105**, 213 (1996).

[58] R. J. Needs, M. D. Towler, N. D. Drummond, P. López Ríos, and J. R. Trail, *J. Chem. Phys.* **152**, 154106 (2020).

[59] K. Szalewicz and H. J. Monkhorst, *J. Chem. Phys.* **75**, 5785 (1981).

[60] E. R. Davidson, S. A. Hagstrom, S. J. Chakravorty, V. M. Umar, and C. F. Fischer, *Phys. Rev. A* **44**, 7071 (1991).